

## Improved Si:As BIBIB Hybrid Arrays

T. HERTER, N. ROWLANDS, S. V. W. BECKWITH, AND G. E. GULL

Department of Astronomy, Cornell University

AND

D. B. REYNOLDS, D. H. SEIB, AND M. G. STAPELBROEK

Rockwell International Science Center

### ABSTRACT

We present results of a program to increase the short wavelength ( $< 10 \mu\text{m}$ ) detective quantum efficiency,  $\eta/\beta$ , of Si:As Impurity Band Conduction arrays. The arrays are epitaxially grown Back-Illuminated Blocked-Impurity-Band  $10 \times 50$  detectors bonded to switched-FET multiplexers. We show that the  $4.7 \mu\text{m}$  detective quantum efficiency increases proportionately with the thickness of the infrared active layer. A BIB array with a thick active layer, designed for low dark current, exhibits  $\eta/\beta = 7\text{--}9\%$  at  $4.7 \mu\text{m}$  for applied bias voltages between 3 and 5 V. The product of quantum efficiency and photoelectric gain,  $\eta G$ , increases from 0.3 to 2.5 as the voltage increases from 3 to 5 V. Over this voltage range, the dark current increases from 8 to  $120 \text{ e}^- \text{ s}^{-1}$  at a device temperature of 4.2 K and is under  $70 \text{ e}^- \text{ s}^{-1}$  for all voltages at 2 K. Because of device gain, the *effective* dark current (equivalent photon rate) is less than  $3 \text{ e}^- \text{ s}^{-1}$  under all operating conditions. The *effective* read noise (equivalent photon noise) is found to be less than 12 electrons under all operating conditions and for integration times between 0.05 and 100 seconds.

### I. INTRODUCTION

Impurity Band Conduction (IBC) detectors and their generic equivalents – Blocked Impurity Band (BIB) and Backside Illuminated Blocked Impurity Band (BIBIB) – were developed to be sensitive to infrared light in the  $6\text{--}26 \mu\text{m}$  wavelength range, but with substantially smaller active volumes than the extrinsic photoconductive detectors normally used at these wavelengths. The smaller active volume means a correspondingly smaller sensitivity to high energy radiation and particles. Silicon BIBs employ a thin, undoped, epitaxially grown silicon layer between a heavily doped, infrared-active layer and a planar contact. The undoped layer blocks hopping conduction (dark current) but conducts the current generated by infrared light which photoionizes neutral impurities in the heavily doped layer. When a voltage is applied between the active layer and the planar contact, the blocking layer causes BIB detectors to behave like reverse-biased diodes rather than

photoconductors. Because of the high doping concentration, BIB detectors achieve good quantum efficiency with an infrared-active layer more than an order of magnitude thinner than that of extrinsic Si photoconductors, making BIBs much less susceptible to damage by cosmic rays. Some of the problems inherent in extrinsic photoconductors are not present in BIBs: there appear to be no large, transient currents associated with voltage changes, and the electrical and optical crosstalk between pixels is small. BIBs offer improved uniformity and larger wavelength coverage than possible with extrinsic photoconductors. The theory and operation of BIBs and the characteristics of the Rockwell International Si BIBIB arrays discussed in this paper are described in detail by Petroff and Stapelbroek (1984, 1985) and Stetson *et al.* (1986).

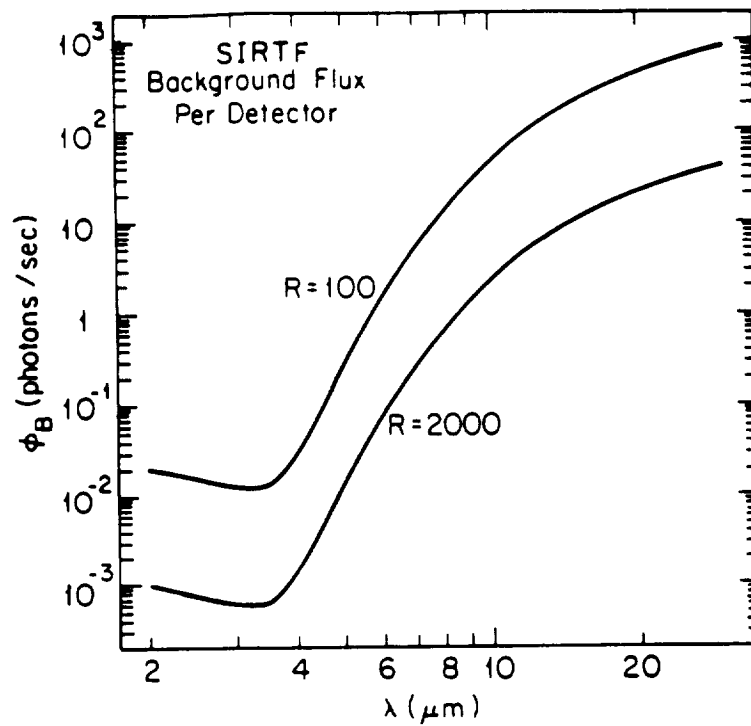
We are developing improved BIB detectors under a program to support the Space Infrared Telescope Facility (SIRTF), a cooled infrared space telescope planned by NASA for launch in 1998. Cornell is building the Infrared Spectrometer (IRS) as one of three instruments for SIRTF. The IRS will provide spectra from 2.5 to 200  $\mu\text{m}$  at resolving powers ( $\lambda/\Delta\lambda$ ) of 100 and 2000. Silicon BIB detectors from Rockwell will cover the 5–27  $\mu\text{m}$  wavelength range for this spectrometer. Because the background radiation from the telescope and celestial sources will be extraordinarily small, the detectors must have good quantum efficiency, low dark current, and low readout noise. A small detector volume is desired to minimize interference from cosmic rays.

Figure 1 shows the background radiation expected at the detector for resolutions of 100 and 2000. The background is dominated by emission from zodiacal dust particles. At the highest resolution, less than one photon per second will reach the detector for wavelengths shorter than 9  $\mu\text{m}$ .

It is evident from Figure 1 that if the IRS is to achieve near background-limited performance, the detectors must be very good and very quiet. It is desirable to simplify the focal plane by using only a few different types of detectors to cover the waveband. The Si:As BIBIB (hereafter simply called BIB) hybrid detector arrays made by Rockwell are the best available to meet these requirements, but the first generation devices have low quantum efficiencies at the short wavelengths,  $\lambda \sim 4 \mu\text{m}$ . We present here results from a program undertaken to improve the short wavelength quantum efficiency of Si BIB detectors.

## II. DETECTOR DESCRIPTION

Detector arrays are produced with 10 rows of 50 pixels. Pixel centers are 150  $\mu\text{m}$  apart, and the detector active area is 135  $\times$  135  $\mu\text{m}$ . The detector array is bump-bonded with indium contacts to a MOSFET multiplexer specially designed for low-noise operation at temperatures of less than 10 K. The photocurrent from each detector is collected at the gate of a MOSFET which can be sampled nondestructively. The nodal capacitance is between 0.37 and 0.42 pf, depending on the detector configuration, and the total capacity is about  $2 \times 10^6$  electrons. The output amplifier of the multiplexer has a gain of 0.7, giving 3.30 to 3.75 electrons per  $\mu\text{V}$ .



**Figure 1:** Photon rate on the midband (5–27  $\mu\text{m}$ ) detectors for resolving powers of 100 and 2000. The transmission of the optics is assumed to be 0.10; the pixel size is  $1.2\lambda/D$ , where  $\lambda$  is the wavelength and  $D$  is the telescope diameter. The major contributor to the photon rate is zodiacal emission which is assumed to have an emissivity of  $2.3 \times 10^{-7}$  and a temperature of 246 K (Hauser *et al.* 1984).

Test results from the first generation of these arrays are presented by Herter *et al.* (1987). The detectors responded poorly to light near 5  $\mu\text{m}$  ( $\eta/\beta \sim 4\%$ ), but otherwise met the requirements for the IRS. A second generation of detectors was made to improve the short wavelength response. The responsivity can be enhanced by increasing the donor concentration and/or by making the infrared active layer thicker. Increasing the donor concentration may increase dark current. Increasing the thickness of the active layer will only be effective if the layer can be fully depleted of ionized donors (due to impurity acceptors) when a voltage is applied to the detector. It is most important to keep the acceptor concentration low.

Rockwell developed a high purity, epitaxial reactor, making it possible to increase the active layer thickness of BIB detectors. A group of detectors was fabricated with different active layer thicknesses and donor concentrations to determine the optimum characteristics for enhancement of short wavelength quantum efficiency while maintaining low dark current. Discrete detectors were cooled to 10 K and illuminated with a photodiode to test performance prior to bonding. The best material was used to make hybrid arrays. Two detector materials were chosen for further evaluation, both with an infrared active

layer twice the thickness of the first generation devices. One was doped uniformly. The other contained a graded donor concentration which increased linearly from the blocking layer to the contact. The average donor concentration was the same for both materials.

Reynolds *et al.* (1988) present initial test results on the responsivity and detective quantum efficiency at 4.5 and 10.6  $\mu\text{m}$  at an operating temperature of 10 K. These tests show that the short wavelength quantum efficiency is a factor of two greater than that of the thin detectors, the same factor as the increase in thickness of the infrared active layer. They found the graded layer device to have the lowest dark current without a loss of responsivity. We present here test results for the graded layer detector operated at 4.2 and 2.0 K. These lower operating temperatures further reduce dark current and are a better match to the range of focal plane temperatures that will be available on SIRTf.

### III. BACKGROUND

#### a) IBC Performance Characterization

The noise,  $N$ , in an IBC device after collecting photons of energy  $h\nu$  for a time  $t$  is:

$$N^2 = \frac{P_B}{h\nu} \frac{\eta}{\beta} (\beta G)^2 t + \beta_d G_d i_d t + R_N^2, \quad (1)$$

where  $P_B$  is the radiant power per  $150 \mu\text{m} \times 150 \mu\text{m}$  area,  $\eta$  is the quantum efficiency,  $G$  is the photoconductive gain,  $\beta (\equiv \langle G^2 \rangle / \langle G \rangle^2)$  is the gain dispersion,  $R_N$  is the readout noise which may be a function of the integration time,  $i_d$  is the dark current,  $G_d$  is the gain of the dark current, and  $\beta_d$  is the gain dispersion of the dark current. In general, we expect  $G_d < G$  and  $\beta_d < \beta$ , since most dark current occurs near the blocking layer. We define the *signal*,  $S$ , to be the number of collected electrons generated by radiation:

$$S = \frac{P_B}{h\nu} (\eta G) t, \quad (2)$$

$$= \frac{P_B}{h\nu} \frac{\eta}{\beta} (\beta G) t. \quad (3)$$

When the fluctuations in the radiation power dominate the last two terms in equation (1), the detective quantum efficiency,  $\eta/\beta$ , may be measured directly from the signal-to-noise ratio:

$$\frac{\eta}{\beta} = \left( \frac{S}{N} \right)^2 \frac{h\nu}{P_B} \frac{1}{t}. \quad (4)$$

Measurement of  $\eta/\beta$  does not require knowledge of the amplifier gain of the device or the nodal capacitance, since these terms affect the signal and noise equally, and thus cancel in the ratio. The quantity  $\eta G$  is determined from the responsivity,  $S/P_B$ , using equation 2. Notice that for photoconductors, the gain dispersion,  $\beta$ , is at least 2 because shot noise in the generation and in the recombination of carriers contribute equally. This factor is typically ignored when quoting the quantum efficiency of photoconductors. Thus, for a photoconductor with  $\eta = 20\%$ ,  $\eta/\beta = 10\%$  which is the relevant quantity for comparison to IBC devices.

### b) Experimental Setup

The detector arrays are cooled in a dual reservoir cryostat filled with liquid helium and nitrogen. By adjusting the pressure over the helium, the detector temperature can be varied between 2 and 4.2 K. The array is illuminated through a 750  $\mu\text{m}$  circular aperture cooled to the detector temperature. A stack of several neutral density and bandpass filters limits the radiation passing through the aperture. For the tests described here, the bandpass filter was centered at 4.7  $\mu\text{m}$  with a width of approximately 0.64  $\mu\text{m}$ . Either an ambient temperature (300 K) metal block with a blackened cavity or a commercial blackbody source was used to illuminate the array through the cooled aperture.

A Stride 460 VMe bus microcomputer controls the array electronics. The Stride microprocessor uses a separate single board computer (SBC) on the VMe bus to provide TTL level clocking signals for the multiplexer. The signals are conditioned with a level-shifter which allows adjustment of both the upper and lower voltages of each clocking pulse. This box also provides steady voltage levels to the array. The array output voltages are amplified through a ten-channel preamplifier with programmable gain and bandwidth. The Stride microprocessor samples the preamplifier output with a multichannel A/D converter which is also on the VMe bus. The level of the output signal from the array is not constant from pixel to pixel. It increases systematically with pixel position across the array, and may saturate the preamplifier or A/D converter. This level change is eliminated by injecting a dynamic offset voltage at the front end of the preamp in synchronization with the array using a D/A converter driven by the SBC.

The array output may be sampled in different sequences to record voltage levels at any time from the beginning to the end of an integration and when the detectors are discharged (reset). We define three sampling schemes which are useful in testing detector characteristics. In the first scheme, called *sequential sampling*, the detectors are read out sequentially at a fixed rate, and the integration time during which charge is collected is proportional to the total time to read the entire array. In the second scheme, called *burst sampling*, all detectors are reset in rapid succession, charge is collected during integration time  $t$ , and the detectors are then sampled sequentially, but very rapidly, so the time to read the array is small compared to the integration time. Either doubly- or triply-correlated sampling may be used with either of these schemes, since the multiplexer allows nondestructive sampling. Triply-correlated sampling can, in principle, remove the kTC noise resulting from fluctuations in the amount of charge left on the detector after reset. In the final scheme, called *sampling up-the-ramp*, each detector is sampled many times during integration. A linear regression fit to the samples determines the rate at which charge accumulates (proportional to the photon rate). This technique typically gives better read noise performance than the other two modes.

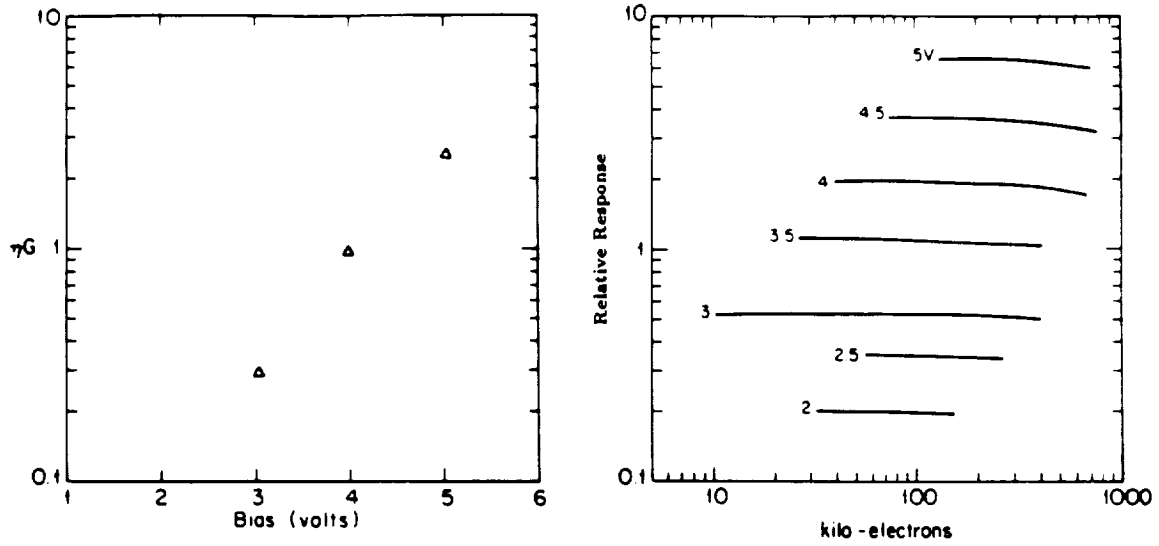


**Figure 2:** Responsivity ( $\eta G$ ) at  $4.7\mu\text{m}$  for a graded profile detector at 4.2 K. The photon rate is  $4000\text{ photons s}^{-1}$  per detector. The responsivity,  $\eta G$ , is computed assuming a fixed nodal capacitance of  $0.37\text{pf}$  independent of detector bias. (a) Responsivity versus bias voltage. (b) Relative responsivities versus collected charge for different bias voltages.

#### IV. TEST RESULTS

We measured the responsivity, detective quantum efficiency, read noise, dark current, transient response, and response to  $\gamma$ -rays to assess detector performance. Because of our interest in the short wavelength quantum efficiency, only measurements at  $4.7\mu\text{m}$  are presented here. The peak detector response occurs at about  $23\mu\text{m}$ .

##### a) Responsivity

Measurements of  $\eta G$  versus bias with the detector operating at 4.2 K are shown in Figure 2a. Figure 2b shows the relative responsivity as a function of collected charge for different bias voltages. The roll-off noted previously by Herter *et al.* (1987) is evident. This effect is likely due to *debiasing* of the detector as charge accumulates.

The responsivity,  $\eta G$ , decreased by factors of 0.6, 0.8 and 1.0 as the detector temperature decreased from 4.2 to about 2 K for operating biases of 5, 4 and 3 volts respectively. The photon background was relatively large compared to the photon background at this wavelength in the SIRTf environment. However, measurements at a lower photon flux of  $\phi_b = 600\text{ s}^{-1}$  show no change in  $\eta G$ .

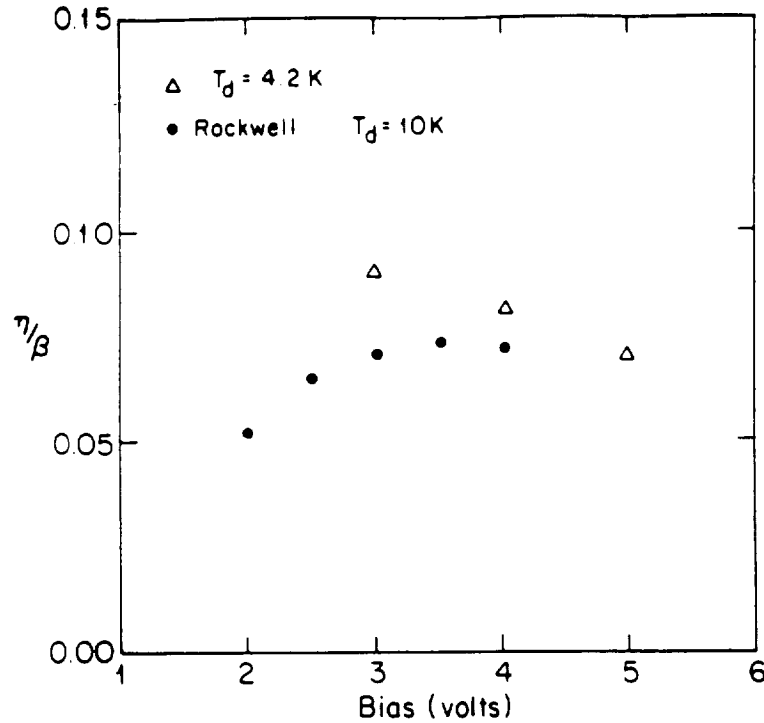


**Figure 3:** Detective quantum efficiency ( $\eta/\beta$ ) at  $4.7\mu\text{m}$  versus bias for the graded profile detector at 4.2 K. The photon rate is  $4000\text{ s}^{-1}$ . Data from Reynolds *et al.* (1988) is also plotted (filled circles).

#### b) Detective Quantum Efficiency

Figure 3 presents the detective quantum efficiency,  $\eta/\beta$ , versus bias voltage. Data from Reynolds *et al.* (1988) are also shown. The array has quantum efficiencies between 7 and 9% depending on bias voltage. Our results are fairly consistent with those of Reynolds *et al.* (1988), who find an optimum value of  $\eta/\beta$  at 3.5 volts. We find that  $\eta/\beta$  continues to increase at lower bias voltages, though the curve could turn over in the voltage region we did not sample. This data set differs from that of Reynolds *et al.*, who operated the array at 10 K, in that our tests were done at 4.2 K. In fact our data indicates that  $\eta/\beta$  increases as the operating temperature decreases and that this effect is greater at the smaller bias voltages. This effect is then completely opposite to the temperature dependence of  $\eta G$  and it would explain the difference between the data in Figure 3. Theoretical modeling (Petroff and Stapelbroek 1984) predicts that at low bias voltages, the active layer will not be fully depleted, and the device quantum efficiency should be low. The quantum efficiency should increase as the depletion of the active layer increases. This is seen in Reynolds *et al.* (1988) data. However, as the device gain increases beyond unity, gain dispersion should cause  $\eta/\beta$  to decline; this is seen in both data sets.

TABLE 1  
READ NOISE PERFORMANCE

Bias (v)	$T_N(e^-)$		$R_N(e^-)$		$R_N(e^-)/\beta G$
	10s	100s	100s	$\beta G$	100s
3.0	55	109	48	4	12
4.0	64	193	34	12	3
5.0	170	620	150	34	4

### c) Read Noise

Table 1 shows the total noise  $T_N$  and read noise  $R_N$ , of the device at integration times of 10 and 100 seconds for different bias voltages; the results include a contribution from dark current noise (see next section) which has to be accounted for in order to determine the read noise. The detector temperature was 4.2 K, and the sampling up-the-ramp scheme provided a measure of the total noise. For most integration times, sampling up-the-ramp gives noises lower by 30 to 50% than either doubly- or triply-correlated sampling. The noise for an individual pixel is determined as the standard deviation of that pixel's value over a sequence of frames (usually five). The total noise (as shown in Table 1) is then the average of the individual pixel deviations. Another method of determining the noise is by subtracting two successive frames and computing the standard deviation of the differences for all pixels in the array. The noises computed with this latter method are therefore a factor of  $\sqrt{2}$  larger than the actual noise for a single frame. This procedure is similar to taking the difference of source and background frames during astronomical observations and might provide a better estimate of the performance during actual use. Also, very low frequency drifts ( $\lesssim 1$  Hz) in the average output level of the array do not affect the noise measured in this manner.

The total noise increases with integration time and with bias voltage, but the read noise is fairly constant with respect to these two quantities, once the noise due to the dark current (see equation 1) is taken into account. The larger read noise seen at a bias of 5 volts is due to the error in subtracting off the noise due to the dark current. This error is large when the dark current noise contributes the vast majority of total. The increase in read noise with integration time as seen by Herter *et al.* (1987) in the first generation devices can be accounted for by the noise due to the dark current and its gain and gain dispersion. Since the BIB has gain (more than one electron per photon), the read noise expressed in equivalent number of detected photons is less than the number shown in Table 1. Because photovoltaic and extrinsic photoconductor detectors have gains at or near unity, the BIB detectors are intrinsically quieter, even if the read noise at the output is the same.

In order to properly evaluate the performance of these detectors for use on SIRTf the read noise should be compared to the noise in the photon background. Thus we should define an *effective* read noise that is the read noise divided by gain and gain dispersion

TABLE 2  
DARK CURRENT PERFORMANCE

Bias (v)	$i_d(e^-/sec)$		$\beta G_d$	$i_d^{eff}(e^-/sec)$	
	2.2°K	4.2°K		2.2°K	4.2°K
4	20	30	12	2	3
5	70	120	30	2	3

( $\beta G$ ) seen by the photons, since the photon noise term is proportional to  $(\beta G)^2$  (see equation 1). The quantity  $\beta G$  is easily determined from the measurements of  $\eta/\beta$  and  $\eta G$ . In fact, when photon noise dominates,  $\beta G$  is given by  $N^2/S$  (see equations 1 and 2). Effective read noises using  $\beta G$  as the scale factor appear in the right-hand columns of Table 1. The effective read noise is quite low.

#### d) Dark Current

Dark currents were measured at both 4.2 and 2 K. Table 2 gives the results. The dark currents are under  $120 e^- s^{-1}$  for all measurements. However, it is the noise contribution of the dark current in comparison to the photon noise contribution that is of interest here. We therefore define an *effective* dark current based on equation 1, which is the dark current multiplied by the  $\beta G$  that applies to the dark current divided by the square of the  $\beta G$  in the photon noise term. The  $\beta G$  for the dark current is determined by evaluating the total noise performance of the darkened array at different integration times. For short integration times the read noise is the major contributor, while at long integration times the dark current term is the major contributor. Then, with value of the dark current known from the accumulated charge, we can determine  $\beta G$  for the dark current. Using our estimates of  $\beta G$  for photons as given in Table 1, and the  $\beta G$  for the dark current given in Table 2, the effective dark current is less than  $3 e^- s^{-1}$  (see Table 2, columns 5 and 6).

#### e) Transient Response

We investigated the temporal response of the detector to changes in the incident photon flux at a bias voltage of 5 V and temperature of 2.2 K. The array was read every 25 ms, and the collected charge was approximately 90,000  $e^-$  per detector per read. A bright source illuminated the array for several seconds, so that each detector received approximately 800,000 electrons per read. Then the illumination was decreased rapidly to 90,000  $e^-$  per read again. The responsivity of the array decreased after the bright illumination for a period extending over many minutes. The responsivity returned to within 5% of the low-level value after 2.5 minutes, and it was within 1% of its initial value after 8 minutes. This behavior does not appear to depend on temperature, but it could be a function of bias voltage and how the detectors are reset. We are investigating these effects and also the responsivity changes for less extreme changes in detector illumination.

#### *f) Radiation Recovery*

The array was irradiated with a  $^{241}\text{Am}$   $\gamma$ -ray source to measure response to high energy radiation. The dominant lines are at 59.54, 17.61, and 13.92 keV which comprise 36, 20 and 13% of the total photon emissions respectively. All other lines are less than 5% of the total. The  $\gamma$ -ray source was about 20 cm from the array illuminating it face-on. In this configuration, a  $\gamma$ -ray is detected by the array every few seconds. The resulting charge on a detector was between a few tens of thousands and a few hundred thousand electrons. The gamma rays do not saturate the detectors. The largest events usually affect three neighboring detectors: the detectors immediately above and below in the same column collect a few times ten thousand electrons, as does the immediately preceding detector in the same row. If there is no infrared illumination on the array, these detectors require about 10 resets to fully recover their response characteristics. The voltage level of the detector in the same row as the pixel primarily affected by the  $\gamma$ -ray actually goes below its normal value when reset immediately after the detection of the  $\gamma$ -ray. The voltage returns to normal after a few more resets.

Since infrared light aided recovery from high energy radiation events, the response was measured using a resistor to illuminate the detector inside the cryostat; no bandpass filter was used. At a frame rate of 10 Hz with a bias voltage of 4 V, the photon background generated 6500 electrons on each detector between resets. The detectors then recovered from radiation events after one reset. At lower photon fluxes, recovery from a radiation hit was similar to that under dark conditions. For 6000  $e^-$  per read and 400  $e^-$  per read, 8 and 12 resets were required, respectively. The low illumination measurements were done at a frame rate of 10 Hz with a 5 volt detector bias. We note that even though the accumulated charge is the same for two of the cases (because of the higher bias), fewer resets are required to recover from an event under high illumination. It is possible that photons anneal the detectors by removing the carriers generated by the  $\gamma$ -hit.

The number of resets after an event appears to determine the recovery time of the detectors. The recovery did not depend on the total time after the event. The radiation response is independent of the detector temperature. We are experimenting with longer integration times (time between resets) and smaller photon fluxes to determine the resulting radiation response under conditions closer to those expected for SIRTf.

### **V. Projected Performance**

Figure 4 shows the projected sensitivity of the SIRTf midband spectrometer using the measured performance characteristics of the Rockwell Si:As BIBIB hybrid array. In this figure we have interpolated our measured  $\eta/\beta$  values of 0.15 and 0.25 for 10 and 18  $\mu\text{m}$  respectively to calculate the curve at various wavelengths. We underestimate the performance at longer wavelengths, since  $\eta/\beta$  increases with wavelength; the peak response occurring near 23  $\mu\text{m}$ . Included for comparison in Figure 4 are the performance curves for ideal detectors with various quantum efficiencies and read noises. An ideal

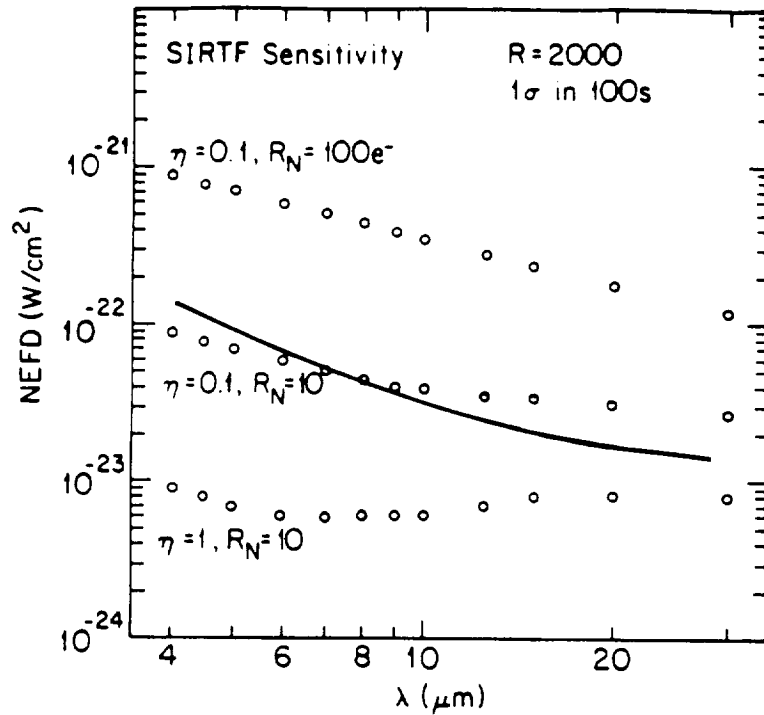


**Figure 4:** Projected performance of the SIRTF midband spectrometer operating at a resolution of 2000 using the measured  $\eta/\beta$ ,  $\eta G$ , dark current and read noise of the Rockwell Si:As BIBIB hybrid array. The  $1\sigma$  sensitivity in 100 s is plotted as a function of wavelength. The array is assumed to be operating at a temperature of 4.2 K and a bias of 4V. Open circles indicate the performance of ideal detectors (no generation-recombination noise and no dark current) with different quantum efficiencies and read noises.

detector here has no dark current, no generation-recombination noise, unity gain, and no gain dispersion. If the measurements obtained here in relatively high backgrounds apply also for the low background conditions of SIRTF, the projected performance using the Si BIBIB array achieves the equivalent performance of an ideal detector with 10% quantum efficiency and a read noise of 10 electrons.

## VI. Conclusions

The short wavelength detective quantum efficiency,  $\eta/\beta$ , of Si BIBIB arrays increases approximately linearly with the thickness of the infrared active layer. The second generation detectors, with twice the active layer thickness, exhibited quantum efficiencies twice those of the first generation detectors. At  $4.7 \mu\text{m}$ , the best detectors have  $\eta/\beta \sim 0.10$ . Furthermore, the dark current is very small in a graded layer device, allowing high bias voltages to increase detector gain. Responsivities,  $\eta G$ , larger than two are seen under

some operating conditions. Because of this gain the *effective* read noise (equivalent number of detected photons) is small, less than 10 electrons. The projected performance of the SIRTf midband spectrometer, 5–27  $\mu\text{m}$ , using the Si BIBIB hybrid arrays is excellent. Sensitivities better than  $10^{-22} \text{ W cm}^{-2}$  can be achieved in 100 s.

Further improvements in  $\eta/\beta$  and  $\eta G$  are possible. The active layer thickness can probably be increased by 30% and remain fully depleted under bias voltage. In addition, Rockwell has demonstrated that anti-reflection coating can improve the responsivity by 20–25% at peak transmission. By coating for 5–6  $\mu\text{m}$ , the responsivity can be improved at the short wavelengths with no degradation or fringing at the longer wavelengths.

On the negative side, the transient performance of the array is not very good. Recovery from changes of state such as background illumination, detector bias, or the detector read out rate require at least 5–10 minutes before stable operation is achieved. This may be a result of the low temperature or low background operating conditions and may only be a characteristic of the graded layer device. In principle, the transient response is not a significant problem for SIRTf conditions because the array can be brought into its required state of operation prior to an exposure. However, recovery from radiation hits could present problems since in the SIRTf high orbit each pixel will be hit about once every 500 seconds. We are currently investigating these issues.

**Acknowledgments:** We are grateful to Jim Houck for useful discussions and for securing the  $^{241}\text{Am}$  source for the radiation testing, and to Justin Schoenwald for providing software support. Financial support for this work was provided by the SIRTf project and Craig McCreight through NASA-Ames contract NAS2-12524 to Cornell University.

## REFERENCES

- Hauser, M. G. *et al.* 1984, *Astrophysical Journal (Letters)*, **278**, L15.
- Herter, T., Fuller, C., Gull, G. E., and Houck, J. R. 1987, "Test Results with Rockwell Si BIBIB Hybrid Arrays," in *Proceedings of Workshop on Ground-based Astronomical Observations with Infrared Arrays*, eds. Wynn-Williams, C. G. and Becklin, E. E., (Univ. of Hawaii, Honolulu), p. 128.
- Petroff, M. D. and Stapelbroek, M. G., "Responsivity and Noise Models of Blocked Impurity Band Detectors," in *Proceedings of the IRIS Specialty Group on Infrared Detectors*, August 1984, Seattle, WA.
- Petroff, M. D. and Stapelbroek, M. G., "Spectral Response, Gain, and Noise Models for the IBC Detectors," in *Proceedings of the IRIS Specialty Group on Infrared Detectors*, August 1985, Boulder, CO.
- Reynolds, D. B., Seib, D. H., Stetson, S. B., Herter, T., Rowlands, N. and Schoenwald, J. 1989, "Blocked Impurity Band Hybrid Infrared Focal Plane Arrays for Astronomy," in *IEEE Transactions on Nuclear Science*, **36**, No. 1, p. 857.
- Stetson, S. B., Reynolds, D. B., Stapelbroek, M. G., and Stermer, R. L., "Design and Performance of Blocked-Impurity-Band Detector Focal Plane Arrays," in *Proceedings of 90th Annual International Technical SPIE Symposium on Infrared Detectors, Sensors, and Focal Plane Arrays*, August 1986, San Diego, CA.